Spatial patterns of glaciers in response to spatial patterns in regional climate

Kathleen Huybers and Gerard H. Roe
University of Washington, Department of Earth and Space Sciences

(Manuscript submitted XXXX, 2007)

Corresponding author address:

Kathleen Huybers
Department of Earth and Space Sciences
University of Washington
Box 351310
Seattle, WA 98195
Tel: 206-543-6229
Email: khuybers@u.washington.edu

Abstract

Glaciers are direct recorders of climate history, and have come to be regarded as emblematic of climate change. They respond to variations in both accumulation and ablation, which can have separate atmospheric controls, leading to some ambiguity in interpreting the causes of glacier changes. Both climate change and climate variability have characteristic spatial patterns and timescales. The focus of this study is the regional-scale response of glaciers to natural patterns of climate variability. Using the Pacific Northwest of North America as our setting, we employ a simple linear glacier model to study how the combination of patterns of melt-season temperature and patterns of annual accumulation produce patterns of glacier length variations. Regional-scale spatial correlations in glacier length variations reflect three factors: the spatial correlations in precipitation and melt-season temperature; the geometry of a glacier and how it determines the relative importance of temperature and precipitation; and the climatic setting of the glaciers (i.e. maritime or continental). With the self-consistent framework developed here, we are able to evaluate the relative importance of these three factors. The results also highlight that to understand the natural variability of glaciers, it is critically important to know the small-scale patterns of climate in mountainous terrain. The method can be applied to any area containing mountain glaciers, and provides a baseline expectation for natural glacier variation, against which the effect of climate changes can be evaluated.

1. Introduction

A major goal in current climate research lies in understanding patterns in climate and how they translate to climate proxies. Glaciers are among the most closely studied of these proxies because they respond directly to both temperature and precipitation variations. A glacier's response to climate is most often characterized by a change in the position of its terminus. Records of terminus advance and retreat are readily available in both the geologic and historic record through the formation of moraines, the study of lichenometry, aerial photography, and satellite imagery. In the absence of temperature and precipitation records, well-dated glacial deposits often serve as the primary descriptor of the climate history of a region.

Despite the direct nature of a glacier's response to climate, the current near-global retreat as well as past glacier variations both present complicated pictures. Though there is evidence that glaciers are presently retreating worldwide (e.g., Oerlemans, 2005), individual glaciers vary in the magnitude of response. In places glaciers are even advancing, as is the case in Norway (e.g., Nesje, 2005). Moreover, some well-documented retreats like that on Mt. Kilimanjaro have complicated causes that are not easily explained (e.g., Molg and Hardy, 2004). While there is often local coherence among glacial advances and retreats, it has proven harder to extrapolate these results across continental-scale regions (e.g., Rupper and Roe, 2008).

The difficulty in interpreting terminus advance and retreat is three-fold. Firstly, glaciers are not indicators of a single atmospheric variable. They reflect the effect of many atmospheric fields, primarily accumulation and temperature, but also cloudiness, wind, and humidity among others. Secondly, each glacier is subject to a particular

combination of the bed slope, accumulation area, debris cover, local shading, etc., creating a setting that is unique to each glacier. Finally, glaciers integrate the interannual variability of the climate over many years or even decades; the advance or retreat of a glacier cannot be traced to a single year's climate.

Hence, in order to understand how spatial patterns in climate variability translate into spatial patterns of glacial response, we must systematically analyze current patterns in regional climate and model a glacier's response to the dominant variables. These patterns of climate variability and glacier response must be understood in order to establish the natural variability of a glacier. It is only when observed responses exceed this expected natural variability that glaciers can be said to be recording a true regional, hemispheric, or global climate change (e.g., Reichert et al., 2002; Roe and O'Neal, 2008).

The goal of this paper is to derive and analyze a model of the expected regional-scale correlations of glacier length variations in response to interannual variability in precipitation and melt-season temperature. We take a first order approach to this problem, using the simplest model framework capable of representing how glaciers amalgamate different aspects of climate to produce terminus variations. In particular, we address the following questions:

1. What are the spatial patterns of variability in precipitation and melt-season temperature?
2. How do these patterns of intrinsic climate variability translate into patterns of glacier advance and retreat?
3. Over what spatial extent can we expect these intrinsic, natural fluctuation of glaciers to be correlated?

We use a simple linear glacier model that has been shown to adequately capture recent glacier variability (Johanneson et al., 1989; Oerlemans, 2005; Roe and O'Neal, 2008). The patterns we find in our results are consistent with those of other glacier mass balance studies (Harper, 1993; Bitz and Battisti, 1999). The advantage of our approach is that it allows us to explore such patterns on a wider, regional scale, and to understand in detail the relative importance of the different causes.

Our modeled patterns of glacier advance and retreat cannot, of course, be directly translated into the paleorecord of glacier advance and retreat because there is no accounting for the processes that build up and deposit moraines on the landscape. These processes are complex and poorly understood (e.g., Putkonen and O'Neal, 2005). We regard our results, therefore, as a means to explore how climate patterns are combined through the dynamical glacier system, and as an aid in the interpretation of glacial landscape features.

2. Setting and Data

Our study area is the Pacific Northwest, covering the northwestern United States, British Columbia, and southern Alaska. This region is ideal because of the large number of well-documented glaciers, the different climatic environments, and the range of glacier sizes that exist in the region. The dominant climate patterns in the area are also well understood. Figure 1 maps the locations of all major glaciers in the region.

Our principal climate data set is that of Legates and Willmott (1990), hereafter denoted LW50, which provides fifty years of worldwide temperature and precipitation station data interpolated onto a 0.5º x 0.5º grid. We distill this dataset into two

atmospheric variables that reflect the most important climatic forcing for glaciers. The first variable is the melt-season temperature, which we define as the average surface temperature between June and September (JJAS). For simplicity, we assume that the ablation rate is directly proportional to the melt-season temperature, as suggested by observations (e.g., Paterson, 1994; Ohmura, 1998). The second variable is the mean annual precipitation, which, again for simplicity, we assume reflects the accumulation of snowfall on a putative glacier within any grid-point. Approximately 80% of precipitation in this region comes in the fall and wintertime (e.g., Hamlet et. al., 2005). The data is linearly-detrended in order to identify the internal variability in these climate variables, and so neglect any recent warming.

These simplifications are appropriate for the first order approach of this study, its focus on the regional-scale response, and the relatively coarse 0.5° resolution data that does not reflect small-scale orographic effects. We discuss refinements of the model framework in the Discussion.

2.1 Climate in the Pacific Northwest

Figures 2a and b depict the mean annual precipitation and the mean melt-season temperature over the region. The Cascade, Olympic, Coast, and St. Elias mountains are important influences on the region's climate. These mountain ranges partition the setting into a generally wet region on the upwind flank of the mountains and a dry region towards the leeward interior. On a smaller scale, not resolved in Figure 2, there are distinct patterns in climate over the peaks and valleys in the mountain ranges, giving rise

to rich and intricate local weather patterns. (e.g., Minder et al., 2007; Anders et al., 2007). We address the important effect of these small-scale patterns in Section 5. For mean melt-season temperature, the pattern is characterized by the north-south gradient, though cooler temperatures at higher elevations can also be seen.

A dominant feature of the atmospheric circulation pattern is the presence of the Aleutian Low. The effects of the dominant modes of climate variability influencing the region (for example, El-Nino (e.g., Wallace et al., 1998), the Pacific Decadal Oscillation (e.g., Mantua et al., 1997), and Pacific North American pattern (e.g., Wallace and Gutzler, 1981)) can all be understood in terms of how they shift the position and intensity of the Aleutian Low. These positional shifts result in a dipole-like pattern, with storms having a tendency to track either north or south, depending on the phase of the mode, and leaving an anomaly of the opposite sign where the storminess is reduced.

The natural year-to-year variation observed in the region's climate system is well characterized by the standard deviations in annual temperature and precipitation from LW50. Figure 2c shows a simple relationship: the interannual variability of precipitation is higher where the mean precipitation is also high. However, for melt-season temperature, the picture is different. Whereas the mean was dominated by the north-south gradient, the variability of melt-season temperature (Figure 2d) is higher inland, reflecting the continentality of the climate.

2.2 Glaciers in the Pacific Northwest

The high precipitation rates and widespread high altitude terrain make this area conducive to the existence of glaciers. The region's glaciers have been extensively

mapped, as have their changes over recent geologic history (e.g., Harper, 1993; Hodge, 1998; O'Neal, 2005; Pelto, 2001; Post, 1971; Porter, 1987; Sidjak, 1999). The glaciers in the region range from the massive tidewater glaciers in southern Alaska to small ice patches in steep terrain. In this study, we focus on the many temperate alpine glaciers in the area because these are the best suited to reflect a clean signature in their response to climate. Even among these temperate glaciers, there is a wide range in size and shape, giving rise to individual variations in advance and retreat.

These advances and retreats cannot be interpreted as responses to long-term climate changes alone. Climate is, by definition, the statistics of weather. In other words, it is the probability density distribution of the full suite of variables that describe the state of the atmosphere over some specified period of interest. A stationary climate, therefore, has constant statistics, with a given mean, standard deviation, and higher-order moments. Glaciers are dynamical systems that integrate up this natural year-to-year climate variability. This integrative quality of glaciers means that even in a constant climate, the length of glaciers will vary on decadal and centennial timescales (e.g., Reichert et. al., 2002; Roe and O'Neal, 2008; Roe, 2008).

3. A Linear Glacier Model

A schematic of the linear model employed in this study is shown in Figure 4. The model is from Roe and O'Neal (2008), which is based on that of Johannesson, et al. (1989). The model assumes that any imbalance between snow accumulation and ice ablation is instantaneously felt as a rate of change at the glacier terminus. Other aspects of the glacier geometry are specified. This model, and similar ones are able to reproduce

realistic glacier variations for realistic climate forcings (Oerlemans, 2001, 2002; Roe and O'Neal, 2008).

Climate is specified by an annual accumulation rate of P (m yr^{-1}) and a melt-season temperature T. Ablation is assumed to be linearly proportional to T, where the constant of proportionality is given by the melt-rate factor, μ. Observations suggest that μ ranges from 0.50 to 0.84 m yr^{-1} $°C^{-1}$ (e.g., Paterson, 1994). The lapse rate, Γ, is taken to be a constant 6.5 ^{o}C km^{-1}.

Let $\overline{L}$ be the equilibrium glacier length that would result from constant $\overline{T}$ and $\overline{P}$, the long-term averages of the melt-season temperature and the precipitation. The model calculates the time evolution of perturbation in glacier length, L', that arises from the interannual anomalies in the melt season temperature, T' and annual precipitation, P'. From here on, we drop the prime symbol, and use L, T, and P to represent the anomalies in length, melt-season temperature and precipitation, respectively.

Roe and O'Neal (2008) show that perturbations in glacier length, L, away from the equilibrium climate state can be described by the following equation:

$$L_{t+\Delta t} = \left(1 - \frac{\mu \Gamma \tan\phi A_{abl} \Delta t}{wH}\right) L_t - \left(\frac{\mu A_{T>0} \Delta t}{wH}\right) T_t + \left(\frac{A_{tot} \Delta t}{wH}\right) P_t \equiv \gamma L_t - \alpha T_t + \beta P_t. \qquad 1$$

The model geometry and parameters are defined in Figure 4, t is time in years and Δt is the interval between successive time steps, which we take to be one year.

Most of the correlations presented in this paper are calculated with respect to Mt. Baker in the Cascade Mountains of Washington state (48.7° N, 121.8° W). Mt. Baker is a large

stratovolcano, flanked by eight glaciers with a broad range of sizes and shapes. Table 1 shows the range in the model parameters and geometry that is reasonable for typical Alpine glaciers in this region, taken from Roe and O'Neal (2008). Ablation areas are calculated from the total area, using the accumulation area ratio (AAR), the ratio of A_{abl} to A_{tot}, which varies from 0.6 to 0.8 in this region (e.g., Porter, 1975). γ ranges between 0.81 and 0.97 (and is unitless), α between 9 and 81 m°C^{-1} and β between 85 and 240 years, depending on the choice of parameters and the size of the glacier. Note that α has the largest uncertainty, due to the large uncertainties in μ and in the *AAR*, both of which, in principle, can be observed and so constrained much better for any specific glacier. Table 1 also shows a standard set of typical parameters, which we use for all calculations from now on unless otherwise stated.

(1) describes a glacier that advances (retreats) if melt-season temperatures are anomalously low (high) or if the accumulation is anomalously high (low). In the absence of any climate anomalies, the glacier returns to its equilibrium length over a characteristic e-folding time scale,

$$\tau \equiv \Delta t/(1-\gamma) = \frac{wH}{\mu\Gamma \tan\phi A_{abl}},$$

which for Mt. Baker glaciers ranges from 5 to 30 years (Table 1).

Roe and O'Neal (2008) show that this linear model is able to capture typical magnitudes of glacier variations in the Cascade Mountains of Washington State, and so is adequate to capture the approximate response of glacier length to large-scale patterns of *P* and *T*. Caveats and possible improvements to the model are noted in the Discussion.

4. Results

4.1 Glacier Correlations

The aim of this study is to explore how patterns of glacier length variations are driven by patterns of climate. From (1) an expression can be derived for the correlation between two glaciers located at two different locations (denoted A and B) in terms of the correlations between *T* and *P*.

$$L_{A,(t+1)} = \gamma_A L_{A,t} - \alpha_A T_{A,t} + \beta_A P_{A,t}, \qquad 2a$$

$$L_{B,(t+1)} = \gamma_B L_{B,t} - \alpha_B T_{B,t} + \beta_B P_{B,t}. \qquad 2b$$

The expected value (denoted by $\langle\ \rangle$) of the correlation between glaciers A and B is

$$\begin{aligned}\left\langle L_{A,(t+1)} L_{B,(t+1)} \right\rangle = {} & \gamma_A \gamma_B \left\langle L_{A,t} L_{B,t} \right\rangle + \alpha_A \alpha_B \left\langle T_{A,t} T_{B,t} \right\rangle + \beta_A \beta_B \left\langle P_{A,t} P_{B,t} \right\rangle \\ & - \gamma_A \alpha_B \left\langle L_{A,t} T_{B,t} \right\rangle + \gamma_A \beta_B \left\langle L_{A,t} P_{B,t} \right\rangle - \alpha_A \gamma_B \left\langle T_{A,t} L_{B,t} \right\rangle + \beta_A \gamma_B \left\langle P_{A,t} L_{B,t} \right\rangle .\end{aligned} \qquad 3$$

Cross terms in temperature and precipitation (i.e. $\left\langle T_{A,t} P_{B,t} \right\rangle$) have been neglected in (3) because calculations show that in this region they are not statistically significant at a 95% confidence level.

$\left\langle L_{A,t} L_{B,t} \right\rangle$ is the covariance of L_A and $L_{B,}$, which is in turn equal to the correlation between L_A and L_B ($\equiv r_{L(A,B)}$), which is our desired answer, multiplied by the standard deviations of L_A and L_B.. The covariances $\left\langle T_{A,t} T_{B,t} \right\rangle$ and $\left\langle P_{A,t} P_{B,t} \right\rangle$ can be calculated from

observations. However, the other terms in (3) are in need of additional manipulation. We elaborate on $\langle L_{A,t} T_{B,t} \rangle$. The other terms can be likewise derived.

From the definition of the correlation between T_A and T_B we can write

$$\langle T_{B,t} \rangle = \sigma_{T,B} \left(r_T \frac{\langle T_{A,t} \rangle}{\sigma_{T,A}} + \left(1 - r_T^2\right)^{1/2} \nu_t \right), \qquad 4$$

where r_t is the correlation of melt-season temperature between points A and B, $\sigma_{T,()}$ is the standard deviation of T at point (), and we assume that the residual, ν_t is a Gaussian-distributed random number of unit variance at time t.

Using the RHS of (4), the value for $\langle L_{A,t} T_{B,t} \rangle$ can be rewritten as

$$\langle L_{A,t} T_{B,t} \rangle = r_T \frac{\sigma_{T,B}}{\sigma_{T,A}} \langle L_{A,t} T_{A,t} \rangle, \qquad 5$$

where we have used the fact that there is no correlation between a random number and $L_{A,t}$. That is $\langle L_{A,t} \nu_t \rangle$=0.

So, to find $\langle L_{A,t} T_{B,t} \rangle$ we need $\langle L_{A,t} T_{A,t} \rangle$. Firstly, T_A can be written in terms of its autocorrelation, $\rho_{T,A}$ and the residuals, which we assume are governed by another Gaussian-distributed white noise process λ_t.

$$T_{A,t} = \rho_{T,A} T_{A,(t-1)} + \left(1 - \rho_{T,A}^2\right)^{1/2} \lambda_t. \qquad 6$$

Therefore using (6) and (2), we can write

$$\langle L_{A,t} T_{A,t} \rangle = \gamma_A \rho_{T,A} \langle L_{A,(t-1)} T_{A,(t-1)} \rangle - \alpha_A \rho_{T,A} \langle T^2_{A,(t-1)} \rangle, \quad 7$$

where again we use the fact that $\langle L_{A,t} \lambda_t \rangle = 0$.

Since the expected value of a distribution of numbers is independent of the time step $\langle L_{A,t} T_{A,t} \rangle = \langle L_{A,(t-1)} T_{A,(t-1)} \rangle$, we rewrite (7) as

$$\langle L_{A,t} T_{A,t} \rangle = \frac{-\alpha_A \rho_{T,A} \sigma^2_{T,A}}{1 - \gamma_A \rho_{T,A}}. \quad 8$$

Therefore the expected correlation between L_t and T_t is a function of the magnitude of T, the autocorrelation of T, and the memory of the glacier.

Finally, inserting the RHS of (8) into (5) yields

$$\langle L_{A,t} T_{B,t} \rangle = \frac{-\alpha_A r_T \rho_{T,A} \sigma_{T,A} \sigma_{T,B}}{1 - \gamma_A \rho_{T,A}}. \quad 9$$

Similar derivations for the remaining terms in (2) yield an equation for the correlation of glacier lengths between A and B.

$$r_{L(A,B)} = \frac{1}{(1 - \gamma_A \gamma_B) \sigma_{L,A} \sigma_{L,B}} \left\{ r_T \alpha_A \alpha_B \sigma_{TA} \sigma_{TB} \left[1 + \frac{\gamma_A \rho_{TA}}{1 - \gamma_A \rho_{TA}} + \frac{\gamma_B \rho_{TB}}{1 - \gamma_B \rho_{TB}} \right] \right. \quad 10$$

$$+r_P\beta_A\beta_B\sigma_{PA}\sigma_{PB}\left[1+\frac{\gamma_A\rho_{PA}}{1-\gamma_A\rho_{PA}}+\frac{\gamma_B\rho_{PB}}{1-\gamma_B\rho_{PB}}\right]\Bigg\}.$$

The terms relating to climate $(r_T, r_P, \sigma_T, \sigma_P, \rho_T, \rho_P)$ can all be calculated from observations.

(10) reveals the dependencies of glacier correlations on both the relationships between climate variables and on the geometries of the glaciers in question. The variables and parameters are: the correlation of the climate variables ($r_{T,P}$); the standard deviations of the glacier length, precipitation, and melt-season temperature ($\sigma_{L,T,P}$); the memory of the glacier and climate ($\gamma, \rho_{T,P}$); and finally the size and shape of the glacier (α, β). We will now discuss each of these factors in turn and how their respective ranges of uncertainty affect the correlations between glaciers.

4.2 The spatial correlation of the climate variables

Spatial correlations between glaciers are fundamentally driven by spatial correlations in the climate: (10) shows that $r_{L(A,B)}$ is equal to a linear combination of $r_{T(A,B)}$ and $r_{P(A,B)}$ From LW50 we calculate at each grid point the correlations of *T* and *P* with their values at Mt. Baker (Figure 4). The thin black line denotes significance at the 95% level, using the Student's t-Test and appropriate number of degrees of freedom at each point (Bretherton et. al. 1999). As expected, r_T and r_P are high in areas surrounding Mt. Baker. However, the spatial extent of significant r_T is much greater than that of r_P. Variations in *T* are dependent on the perturbations in the summertime radiation balance,

which appear to be fairly uniform over the region.

A striking feature of r_P is the antiphasing between Washington and southeastern Alaska. The dipole pattern results from the tendency of storms to be more prevalent in one of the two regions, leaving the other relatively dry. The smaller area of significant values of r_P reflects the smaller spatial scale of precipitation patterns.

4.3 The relative importance of T and P for a glacier.

While the correlations in T and P are the main factors in correlations in L, the relative importance of T or P for glacier length also matters. In what follows, we determine the ratio of length variations forced only by T (denoted as $\sigma_{L,T}$) to length variations forced only by P (denoted as $\sigma_{L,P}$).

These expressions can be derived from (1). Setting P=0, the expected value of a glacier forced only by T is

$$\left\langle L_{t+1}^2 \right\rangle = \gamma^2 \left\langle L_t^2 \right\rangle + \alpha^2 \left\langle T_t^2 \right\rangle - 2\gamma\alpha \left\langle L_t T_t \right\rangle. \qquad 11$$

Using our derivation for $\left\langle L_t T_t \right\rangle$ from (8), the variance of the expected length can be written

$$\sigma_L^2 = \gamma^2 \sigma_L^2 + \alpha^2 \sigma_T^2 + \frac{2\gamma\alpha^2 \rho_T \sigma_T^2}{1 - \gamma\rho_T}. \qquad 12$$

Rearranging (12), the standard deviation for a glacier forced only by T' is

$$\sigma_{L,T} = \alpha_T \sigma_T \sqrt{\frac{1}{1-\gamma^2}\left(1+\frac{2\gamma\rho_T}{1-\gamma\rho_T}\right)}. \qquad 13$$

Similarly the expression for a glacier forced only by *P* is

$$\sigma_{L,P} = \beta_P \sigma_P \sqrt{\frac{1}{1-\gamma^2}\left(1+\frac{2\gamma\rho_P}{1-\gamma\rho_P}\right)}. \qquad 14$$

The ratio, *R,* between the two is therefore

$$R = \frac{\sigma_{L,T}}{\sigma_{L,P}} = \frac{\alpha}{\beta}\frac{\sigma_T}{\sigma_P}\sqrt{\frac{1+\frac{2\gamma\rho_T}{1-\gamma\rho_T}}{1+\frac{2\gamma\rho_P}{1-\gamma\rho_P}}}. \qquad 15$$

From (1), $\frac{\alpha}{\beta}$ can be rewritten as $\mu A_{T>0}/A_{tot}$, and therefore (15) can also be written:

$$R = \frac{\sigma_{L,T}}{\sigma_{L,P}} = \frac{A_{T>0}}{A_{tot}} \cdot \frac{\mu\sigma_T}{\sigma_P} \cdot \sqrt{\frac{1+\frac{2\gamma\rho_T}{1-\gamma\rho_T}}{1+\frac{2\gamma\rho_P}{1-\gamma\rho_P}}}. \qquad 16$$

The terms $\frac{2\gamma\rho_T}{1-\gamma\rho_T}$ and $\frac{2\gamma\rho_P}{1-\gamma\rho_P}$ in (15) and (16) are similar to one another. Because γ is always less than one, and calculations (not given) show that values for $\rho_{T,P}$ are typically close to 0.2-0.3, the ratio of these terms will be close to one.

In order to convey a clear sense of the regional coherence of glacier patterns, we present our analyses as if there were a glacier at each grid point in the figure. In other words, we imagine that within each grid point in the LW50, there is a piece of topography high enough to support glaciers. This is simply a device for clarity of presentation – comparison with real glaciers comes directly from Figure. 1.

Figure 5a shows *R* for the standard set of parameters. To convey a sense of the uncertainty in *R*, we also combine the highest melt rate with the lowest AAR and the lowest melt rate with the highest AAR (Figures 5b and c). Overall the calculations suggest that over most of the area glaciers are more sensitive to melt-season temperature than to precipitation, except for a narrow coastal band where glaciers are always more sensitive to *P*, because of the high precipitation variability and muted melt-season temperature variability (i.e., Figure 2). However the extent of *T* dependence varies greatly depending on the choice of parameters. Glaciers with a high melt-factor or a large ablation area, are much more likely to be affected by variations in *T*. In Section 5 we explore how small-scale patterns of climate, not resolved at this scale, can affect this answer.

4.4 Standard Deviations

From (10) it can be seen that the standard deviation of *T* or *P* and the standard deviation of *L* affect $r_{L(A,B)}$ directly. Because σ_T and σ_P also strongly influence the

sensitivity of a glacier's length changes (section 4.3.2) their magnitudes can greatly increase or decrease the importance of R and σ_L.

We derive a formula for σ_L from the root of the sum of the squares of (13) and (14) :

$$\sigma_L = \left\{ \frac{1}{1-\gamma^2} \left[\alpha^2 \sigma_T^2 \left(1 + \frac{2\gamma\rho_T}{1-\gamma\rho_T} \right) + \beta^2 \sigma_P^2 \left(1 + \frac{2\gamma\rho_P}{1-\gamma\rho_P} \right) \right] \right\}^{1/2}. \qquad 17$$

Figure 6 shows σ_L for standard parameters. Values range from 100 to over 300 m. σ_L is high along the coasts, where σ_P is also high. Southeast British Columbia also has above average values in σ_L, corresponding to high values in σ_T.

4.5 Correlations between glaciers with the same geometry

We now apply (9) at to each grid-point in LW50 and correlate a glacier at that point with a glacier that rests on Mt. Baker. We begin by imposing the same γ,α, and β at each point, taking values which are characteristic for a typical glacier (Table 1), in order to eliminate differences in correlation due to geometry, and thus isolate the effect of spatial patterns in climate. The effect of differences in geometry and choices in parameters will be addressed in the following section.

Figure 7 shows the expected correlations between a theoretical glacier at each point and a glacier resting on Mt Baker. The correlations between glaciers are strongest where both T and P are well correlated with Mt. Baker. r_L is also high on the southeast coast of Alaska, where P is most strongly anti-correlated with Mt. Baker and where the

glaciers are most sensitive to *P*. These results are consistent with those of Bitz and Battisti (1999). There are also regions where *T* dominates. For example, the strong sensitivity to *T* northeast of Mt. Baker (Figure 5), and where r_T is also high (Figure 4b) also gives rise to strong glacier correlations. Little to no correlation can be expected in regions where both the *T* and *P* correlations are low and the value of *R* is ambiguously close to one, such as is the case in the Northwest Territories of Canada.

Inferences of the spatial extent of past climate changes are often made by comparing the reconstructed dates of relict moraines. Given the point made in this study, that regional correlations in glaciers also arise from natural interannual variability alone (i.e. in a constant climate), there is some chance that concurrent advances would be misinterpreted. Furthermore, the statistical significance of a hypothesized change in climate is difficult to establish from the few points that are typically available from even well-dated moraines. The integrative nature of a glacier gives it a memory of previous climate states and means that the number of independent observations is much lower than the number of years in a record. In the appendix, we show calculations for deriving the appropriate number of degrees of freedom using our model, given the autocorrelation of both the glaciers and the *T* and *P* values.

4.6 Correlations between Glaciers with Differing Geometries

Assuming that all glaciers have the same geometry is clearly a simplification. We expect the spatial correlation between glaciers to weaken if we compare glaciers of different geometries. Because we cannot present the full range of glacier geometries at every point, we focus on grid points that have a few key climate locations. These

locations are shown in Figure 4b, and were chosen to encompass as large a range as possible for this region of r_P, r_T, and R values, and which are detailed in Table 2.

We consider five combinations of glacier parameters (the five main glaciers of Mt Baker, given in Table 1), and three values for the *AAR* at each of the five points. We then correlated the terminal advance and retreat with that of a typical glacier on Mt. Baker, with an *AAR* of 0.7 and a μ of 0.67 m $yr^{-1}°C^{-1}$ The values of r_L calculated with respect to Mt. Baker , as well as r_T and r_P are shown in Figure 8.

The correlations are strikingly insensitive to this range of parameter variations. r_T and r_P are the main drivers of the correlation between glaciers. Differences in the basic geometry are of secondary importance. To the extent that parameters do matter, the variations in the *AAR* and μ are, of most importance (Also Roe and O'Neal, 2008).

5. Small-scale patterns

While the LW50 dataset has the advantage of a long record, it lacks the small-scale detail of climate patterns due to individual mountain peaks and valleys that strongly influences the behavior of individual glaciers. Since 1997 the fifth generation Penn State-National Center for Atmospheric Research Mesoscale model (known as the MM5, (Grell et al. (1995)) has been run (by the Northwest Regional Modeling Consortium at the University of Washington) at 4 km horizontal resolution over the Pacific Northwest (Mass et. al. 2003; Anders et al., 2007; Minder et al., 2007). Though the short interval of the model output makes statistical confidence lower, it is instructive to look at the patterns of temperature and precipitation over the region on such a fine grid, and repeat the calculations we have performed using LW50. Roe and O'Neal (2008) find good

correspondence between the MM5 output and SNOWTEL observations in the vicinity of Mt. Baker. The performance of the MM5 model in this region, relative to observations, has also been evaluated by Colle et al. (2000).

The patterns in the mean annual precipitation in Washington State (Figure 9a) is dominated by the Olympic and Cascadian mountains. Localized maxima in precipitation near individual volcanic peaks can be identified. The pattern of interannual variability of annual precipitation, measured by the standard deviation, is similar to the pattern of the mean, Mean melt-season temperatures in the region (Figure 9b) are dominated by elevation differences, with colder temperatures recorded in the mountains. Interannual variability in the mean melt-season temperature, on the other hand, is fairly uniform over the region (Figure 9d). but the amplitude is increased somewhat and exceeds 1 m yr^{-1} in places (Figure 9b).

Using (15), the spatial pattern in R can be plotted for the standard set of parameters (Figure 10). Due to the high interannual variability in annual precipitation, the variability of glaciers in the Cascades and Olympic mountains is predicted to be most sensitive to variability in precipitation. This is confined to the high elevations. Lower elevation points, dominated by temperature variability, are not able to sustain actual glaciers in the modern climate, due to their relatively low elevations.

The high levels of precipitation variability in the mountains also drive high values of the standard deviation in glacier length, exceeding 1400 m in places (Figure 11). By definition of the standard deviation, the glacier would spend approximately 30% of its time outside of the $\pm 1\sigma$. Thus over the long-term, fluctuations of two to three kilometers in glacier length should be expected, driven solely by the interannual variability inherent

to a constant climate (Roe and O'Neal, 2008). This result highlights the crucial importance of knowing small-scale patterns of climate in mountainous regions in determining the response of glaciers.

On this spatial scale, interannual climate variations from the MM5 model output are very highly correlated in space, which can also be seen in Figure 7. This translates into very high spatial correlations in glacier response (not shown).

6. Summary and Discussion

A simple linear glacier has been combined with climate data to address how regional-scale patterns in precipitation and melt-season temperature combine to produce regional-scale patterns in glacier response. In our model framework, correlations in the glacier lengths are a linear combination of the spatial correlations in the climate variability. The climate correlations are modified by the relative importance of temperature and precipitation to the glacier response, which in turn is a function of the glacier geometry and mass balance parameters.

In coastal regions high precipitation variability and low melt-season temperature variability mean the patterns of glacier response are controlled by the patterns of precipitation variations. Conversely in continental climates, glacier patterns are most influenced by the patterns in melt-season temperature. Results are quite insensitive to variations in glacier geometry – it is the spatial patterns in T and P that are the key drivers of spatial patterns in glacier variations.

Finally, using seven years of archived output from a high-resolution numerical weather prediction model shows that the increased total precipitation and precipitation

variability characteristic on individual coastal mountain peaks will give rise to large variation in glacier advance and retreat.

The correlations that are calculated in this study are derived using a simple model and a grid size that is larger than the area of a single glacier, and so should be regarded as providing insight and not predictions. In exchange for being able to understand and analyze the results of the system, we have neglected many of the complications that exist in true dynamical glacier systems and mountain climates. We feel confident that our choice in LW50 is adequate, as the North American Regional Reanalysis model and the ERA40 grid-spaced dataset produced very similar results. However, climate data at 0.5° resolution cannot capture the full gamut of climatic effects in mountainous terrain. Also, we opted to present results in terms of the correlation between glaciers. An alternative would have been to calculate empirical orthogonal functions (EOFs) – to find the modes that account for the largest proportion of the variance in glacier advance and retreat. Different treatments for the mass balance are also possible: we could have chosen to use a positive degree-day model (e.g., Braithwaite and Zhang, 1999) or a full surface energy balance model (e.g., Rupper, 2007) to calculate glacier mass balance. The assumption that all precipitation becomes accumulation could be relaxed by including a temperature-dependent threshold for snow.

We have also made significant assumptions regarding glacial processes. Chief among these assumptions is the neglect of glacier dynamics. However several studies have shown that the linear model is capable of reproducing reasonable variations in glacier length (e.g., Johanneson et al., 1989; Oerlemans, 2005; Roe and O'Neal, 2008), and so is adequate for the purposes of the present study. Glacier geometry is also highly

simplified in the linear model. Tangborn et. al. (1990) concluded that area distribution of each glacier was the main distinguishing characteristic accounting for difference in mass balance on two adjacent glaciers in the North Cascade range of Washington State between 1947 and 1961, highlighting the complexities in small scale geometric and climatic factors relevant to glaciers.

Lastly, we have focused on glaciers where the connection with temperature and precipitation is clear and well understood. Our framework cannot be directly applied to tropical or tidewater glaciers, glaciers with a history of surging, or large ice caps or ice sheets, where the physics of that connection is more complex. Further work should be performed understanding not only spatial patterns in glacial correlation, but temporal patterns as well. The model can also readily be used to evaluate when and where a climatic trend in glacier length can be detected against the background interannual climatic variability.

Acknowledgements

We thank Michael O'Neal, Summer Rupper, and Eric Steig for stimulating conversations, and Justin Minder and Cliff Mass for supplying the MM5 data. The work was funded by National Science Foundation under grant #0409884..

References

Anders, A.M., G.H. Roe, D.R. Durran, and J.R. Minder, 2007: Small-scale spatial gradients in climatological precipitation on the Olympic Peninsula. *J. Hydrometeorology, 8*, 1068-1081.

Braithwaithe, R.J., and Y. Zhang, 2000: Sensitivity of mass balance of five Swiss glaciers to temperature changes assessed by tuning a degree-day model. *J. Glaciology*, **46**, 7-14.

Colle, B. A., C. F. Mass, and K. J. Westrick, 2000: MM5 precipitation verification over the pacific northwest during the 1997–99 cool seasons. *Weather and Forecasting*, **15**, 730–744.

Hamlet, A.F., Mote, P.W., M.P. Clark, and D.P. Lettenmaier, 2005: Effects of precipitation and temperature variability on snowpack trends in the western United States, *J. Climate*, **18**,4545-4561.

Harper, J. T., 1993: Glacier Terminus Fluctuations on Mount Baker, Washington, USA, 1940-1990 and Climatic Variations. *Arctic and Alpine Research*, **25**, 332-340.

Harrison, W.D., D.H. Elsberg, K.A. Echelmeyer, and R.M. Krimmel, 2001: On the characterization of glacier response by a single time-scale. *J. Glaciology*, **47**, 659-664.

Hodge, S. et.al. Climate Variations and Changes in Mass of Three Glaciers in Western North America, 1998: *J. Climate*, **11**, 2161-2179.

Legates, D.R, and C.J. Willmott, 1990: Mean Seasonal and Spatial Variability in Global Surface Air Temperature. *Theoretical Applications of Climatology*, **41**, 11-21.

Legates, D.R. and C.J. Willmott, 1990: Mean Seasonal and Spatial Variability in Gauge-Corrected, Global Precipitation. *Int. J. Climatology*, **10**, 111-127.

Mantua, N.A, S.R. Hare, Y. Zhang, J.M. Wallace, and R.C. Francis, 1997: Pacific interdecadal climate oscillation with impacts on salmon production. *Bull. Amer. Met. Soc.* **78***,* 1069-1079.

Minder, J.M., D.R. Durran, G.H. Roe, and A.M. Anders, 2008: The climatology of small-scale orographic precipitation over the Olympic Mountains: patterns and processes. *Quartely J. Roy. Met. Soc., in press.*

Molg, T. and D.R. Hardy, 2004: Ablation and associated energy balance of a horizontal glacier surface on Kilimanjaro. *J. Geophys. Res.*, **109**, doi10.1029/2003JD004338.

Nesje, A., 2005: Briksdalsbreen in western Norway: AD 1900-2004 frontal fluctuations as a combined effect of variations in winter precipitation and summer temperature. *The Holocene,* **15**; 1245

Oerlemans, J., 2005:Extracting a Climate Signal from 169 Glacier Records. *Science*, **308**, 675-677.

Oerlemans, J., 2001: *Glaciers and Climate Change*, A. A. Balkema Publishers, Rotterdam, Netherlands. 160 pp.

Ohmura, A., and M. Wild, 1998: A possible change in mass balance of Greenland and Antarctic ice sheets in the coming century. *J. Climate,* **9,** 2124-2135.

O'Neal, M.A., 2005: Late Little Ice Age glacier fluctuations in the Cascade Range of Washington and northern Oregon. Dissertation, University of Washington. pp. 117.

Paterson, W.S.B., 1994: *The Physics of Glaciers*, 3rd ed. Elsevier Science.

Pelto, M. and C. Hedlund, 2001: Terminus behavior and response time of North Cascade glaciers, Washington, USA . *J. Glaciology*, **47**, 497-506.

Porter, S., 1978: Present and past glaciation threshold in the cascade range, Washington, USA: topographic and climatic controls and paleoclimate implications. *J. Glaciology*, **18**, 101-116.

Post, A., D. Richardson, W.V. Tangborn, and F.L. Rosselot, 1971: Inventory of glaciers in the North Cascades, Washington. USGS Prof. Paper, 705-A, 1971.

Reichert, B.K., L. Bengtsson, and J. Oerlemans, 2002: Recent Glacier Retreat Exceeds Internal Variability. *J. Climate*, 3069 – 3081.

Roe, G.H., 2008: Feedbacks, time scales, and seeing red. *Annual Reviews Earth and Planetary Sciences, in review.*

Roe, G.H. and M.A. O'Neal, 2008: The response of glaciers to intrinsic climate variability: observations and models of late Holocene variations in the Pacific Northwest. *In review.*

Rupper, S.B., and G.H. Roe, 2008: Glacier changes and regional climate – a mass and energy balance approach. *J Climate, in press.*

Sapaino, J.J., W.D. Harrison, and K.A. Echelmeyer, 1998: Elevation, volume and terminus changes of nine glaciers in North America. *J. Glaciology*, **44**, 119-135.

Sidjak, R.W., and R.D. Wheate, 1999: Glacier mapping of the Illecillewaet icefield, British Columbia, Canada, using Landsat TM and digital elevation data. *Int. J. Remote Sens.*, **20**, 273 – 284.

Tangborn, W.V., Fountain, A.G., and W.G. Sikonia, W.G., 1990: Effect of area distribution with altitude on glacier mass balance – a comparison of north and south klawatti glaciers, Washington state, USA. *Annals of Glaciology,* **14**, 278-282.

Wallace, J.M. and D. Gutzler, 1981. Teleconnections in the Geopotential Height Field during the Northern Hemisphere Winter. *Mon Weather Rev.*, **109**, 784-812.

Wallace, J.M., E.M. Rasmussen, T.P. Mitchell, V.E. Kousky, E.S. Sarachik, and H. von Stoch, 1998: On the structure and evolution of ENSO-related climate variability in the tropical Pacific: lessons from TOGA. *J. Geophys. Res*., **103**, 14,241-14,259.

Appendix

The autocorrelation of a glacier significantly constrains the number of degrees of freedom (d.o.f) available to qualify the significance of an observed r_L. The greater the timescale, the more a glacier is influenced by its previous states, and so the fewer statistically independent observations that are obtainable in a given interval of time. This glacier memory increases the likelihood that simply by chance, high correlations will be observed between glaciers. To calculate the correct number of d.o.f. for a given length of time, and so to derive proper confidence intervals, we must also derive an equation for ρ_L.

The autocorrelation of the length is described by finding the covariance between the lengths from one time step to the next

$$\langle L_{t+1}L_t\rangle = \gamma^2\langle L_tL_{t-1}\rangle + \alpha^2\langle T_tT_{t-1}\rangle + \beta^2\langle P_tP_{t-1}\rangle + \gamma\alpha\langle L_tT_{t-1} + L_{t-1}T_t\rangle + \gamma\beta\langle L_tP_{t-1} + L_{t-1}P_t\rangle. \quad (1)$$

Multiplying (1a) by T_{t-1} and again neglecting the cross terms between *T* and *P,*

$$\langle L_tT_{t-1}\rangle = \gamma\langle L_{t-1}T_{t-1}\rangle + \alpha\langle T_{t-1}^2\rangle. \quad (2)$$

Utilizing (7 (from the main document)) yet again, to replace $\langle L_{t-1}T_{t-1}\rangle$, the length at any given time is related to *T* at that point at the previous time step.

$$\langle L_tT_{t-1}\rangle = \frac{\gamma\alpha\rho_T\sigma_T^2}{1-\gamma\rho_{TA}} + \alpha\sigma_T^2. \quad (3)$$

Because *T* at time *t* can be related to temperature at time *t-1* via its autocorrelation ρ_T^2 at that point, plus random component (see (5 in main document)), we write

$$\langle L_{t-1}T_t\rangle = \frac{\alpha\rho_T^2\sigma_T^2}{1-\gamma\rho_{TA}}. \quad (4)$$

Using this same derivation for $\langle L_t P_{t-1} + L_{t-1} P_t \rangle$, we enter (3) and (4) into (2). Our equation describing the autocorrelation of the length of the glacier is written as:

$$\rho_L = \frac{1}{\sigma_L^2 (1-\gamma^2)} \left\{ \alpha^2 \rho_T \sigma_T^2 \left[1 + \frac{\gamma^2}{1-\gamma\rho_T} + \frac{\gamma}{\rho_T} + \frac{\gamma\rho_T}{1-\gamma\rho_T} \right] \right. \tag{5}$$

$$\left. + \beta^2 \rho_P \sigma_P^2 \left[1 + \frac{\gamma^2}{1-\gamma\rho_P} + \frac{\gamma}{\rho_P} + \frac{\gamma\rho_P}{1-\gamma\rho_P} \right] \right\}.$$

If the autocorrelations in the climate $\rho_{T,P}$ are zero, (5) will simplify dramatically.

This autocorrelation allows us to determine the value that we should input into Bretherton et. al's (1999) value to for determining the correct number of d.o.f. in a time series, given some level of autocorrelation. The autocorrelation of the glacial system requires far more yearly time steps in order to determine a significant correlation than its forcings, which have a much shorter memory.

Therefore, we increase the numbers of d.o.f. by assuming that the 1950-199 detrended values for temperature and precipitation are representative of the range of variation over longer periods of time. This is a reasonable assumption as the brevity of the detrended *T* and *P* data yields a conservative estimate of the climate variations.

Table 1: Values for geometric parameters that are put into (1) for five glaciers on Mount Baker, Washington (Roe and O'Neal, 2008). For the values shown here an accumulation-area ratio (*AAR*) of 0.7 was assumed. A_{tot} is the total glacier area (m^2); A_{abl} is the area over which the glacier ablates (m^2); μ is the melt-rate factor (a standard value of 0.67, and a range of 0.5 to 0.84 m yr^{-1} C^{-1} was used); Γ is the atmospheric lapse rate (6.5 C km^{-1}); ϕ is the slope of the bed; τ is the e-folding relaxation timescale (yrs); γ (unitless), α (m C^{-1}), and β (yrs) are combinations of the above variables, as prescribed in (1).

	Boulder	**Deming**	**Coleman**	**Easton**	**Rainbow**	**'Typical'**
A_{tot} (km^2)	4.30	5.4	2.1	3.6	2.7	4.0
A_{abl} (km^2)	1.3	1.6	0.64	1.1	0.81	1.2
$\tan\phi$	0.47	0.36	0.47	0.34	0.32	0.4
w (m)	550	450	650	550	300	500
H (m)	50	50	39	51	47	50
τ (yrs)	10	9	20	17	13	12
γ	0.90	0.89	0.95	0.94	0.92	0.92
α (m $^oC^{-1}$)	32	48	17	26	39	77
β (yrs)	160	240	85	130	190	160

Table 2: Key points to correlate with Mt. Baker over a variety of glacier geometries. This table lists the latitude and longitude of each point, as well as the correlations in precipitation (r_P) and temperature (r_T), and the sensitivity ratio (R). See Fig. 9.

point	**lat**	**lon**	**nearest mountain**	r_P	r_T	R
A	47.3 N	123.7 W	Olympus	0.85	0.92	0.39
B	49.8 N	120.2 W	Girabaldi	0.75	0.82	2.10
C	53.3 N	116.8 W	Columbia Icefield	0.40	0.26	2.00
D	46.3 N	119.8 W	Adams	0.19	0.85	2.40
E	60.3 N	142.7 W	Wrangell	-0.37	0.22	0.41

Figure Captions

Figure 1. Glaciers in the Pacific Northwest shown in red. Data from the global land ice monitoring from space (GLIMS) project (http://www.glims.org/_ The location of Mt Bake is denoted with an asterisk. Also indicated in the figure are the locations where glacier model sensitivity is tested. Figure courtesy Harvey Greenberg).

Figure 2. Climate mean and variability in the Pacific Northwest from LW50. a) Mean annual precipitation, in m yr^{-1}; b) Mean melt-season (JJAS) temperature in °C; c) interannual standard deviation of mean annual precipitation, in m yr^{-1}; and d) interannual standard deviation of melt-season temperature, in °C.

Figure 3: Schematic of linear glacier model, based on Johanneson et. al. (1989). Precipitation falls over the entire surface of the glacier (A_{tot}). Melt is linearly proportional to the temperature, which, in turn, decreases linearly as the tongue of the glacier recedes up the linear slope (tan ϕ), and increases as the glacier advances downslope. Melt occurs over the lower reaches of the glacier where melt-season temperature exceeds 0 ($A_{T>0}$), and net mass loss occurs over a smaller area where melting exceeds precipitation (A_{abl}), The upper boundary of this latter region is known as the equilibrium line altitude, (ELA). The height (H) of the glacier, and the width of the ablation area (w) remain constant by assumption.

Figure 4. a) Correlation in annual mean precipitation between each grid point and Mt. Baker, from LW50 dataset. Note the dipole of correlations between Alaska and

Washington.; b) as in a), but for the correlation of melt-season temperature. Note the widespread correlation of uniform sign over the region. Correlations exceeding about 0.28 would pass a t-test at greater than 95% confidence.

Figure 5. Ratio of sensitivities to temperature and precipitation for a typical glacier geometry at each grid point, for different choice of model parameters. Warm colors denote temperature sensitivity, while cool colors denote sensitivity to precipitation. Panel a) has the standard parameters. Panel b) has the largest ablation area and melt rate factor, and panel c) has the smallest values of the ablation area and melt rate factor.

Figure 6: Standard deviations of glacier length at each grid point if a typical glacier exists at each grid point. Standard deviations are calculated from (17). Large standard deviations in length are driven by large standard deviations in either precipitation or temperature (compare with Figure 2).

Figure 7: Correlations between a typical glacier glacier at each grid point and at Mt. Baker, calculated from (9).

Figure 8: Sensitivity test of correlations at selected locations (see Figure 5b), to varying the glacier geometry and parameters. T and P denote melt-season temperature and annual precipitation correlations, respectively, between that location point and Mt. Baker. The colored symbols represent the correlation of glacier length between that location and Mt. Baker, and the range arises from using the five different parameter sets applying to the

different Mt. Baker glaciers (given in Table 1)., Finally the different colors mean a different AAR was used: green (AAR =0.6), red (AAR = 0.7), and (AAR = 0.8).

.

Figure 9: Archived output from MM5 numerical weather prediction for the Pacific Northwest at 4 km scale: a) Mean annual precipitation; b) Mean melt-season temperature; c) Standard deviation of precipitation; and d) standard deviation of melt-season temperature. Contours of the model surface elevation are also plotted every 500 m, and the location of Mt. Baker is indicated with an asterisk. Note the small-scale patterns of climate associated with the mountainous terrain, in particular the high rates of orographic precipitation.

Figure 10. The ratio of sensitivities to temperature and precipitation of a glacier length with a typical Mt. Baker-like geometry, calculated at every model grid point from (16). Blue indicates a greater sensitivity to precipitation. The mountainous regions of the Olympics and Cascades, where glaciers in the region actually exist, are dominated by sensitivity to variation in the precipitation.

Figure 11: The standard deviation of glacier length calculated from (17) using the 4 km resolution MM5 output. This fine-resolution scale shows that in the mountainous regions where glaciers exist, the standard deviation in glacier length is much higher than in the lower elevations. The high standard deviations are driven by the high variability in precipitation there.

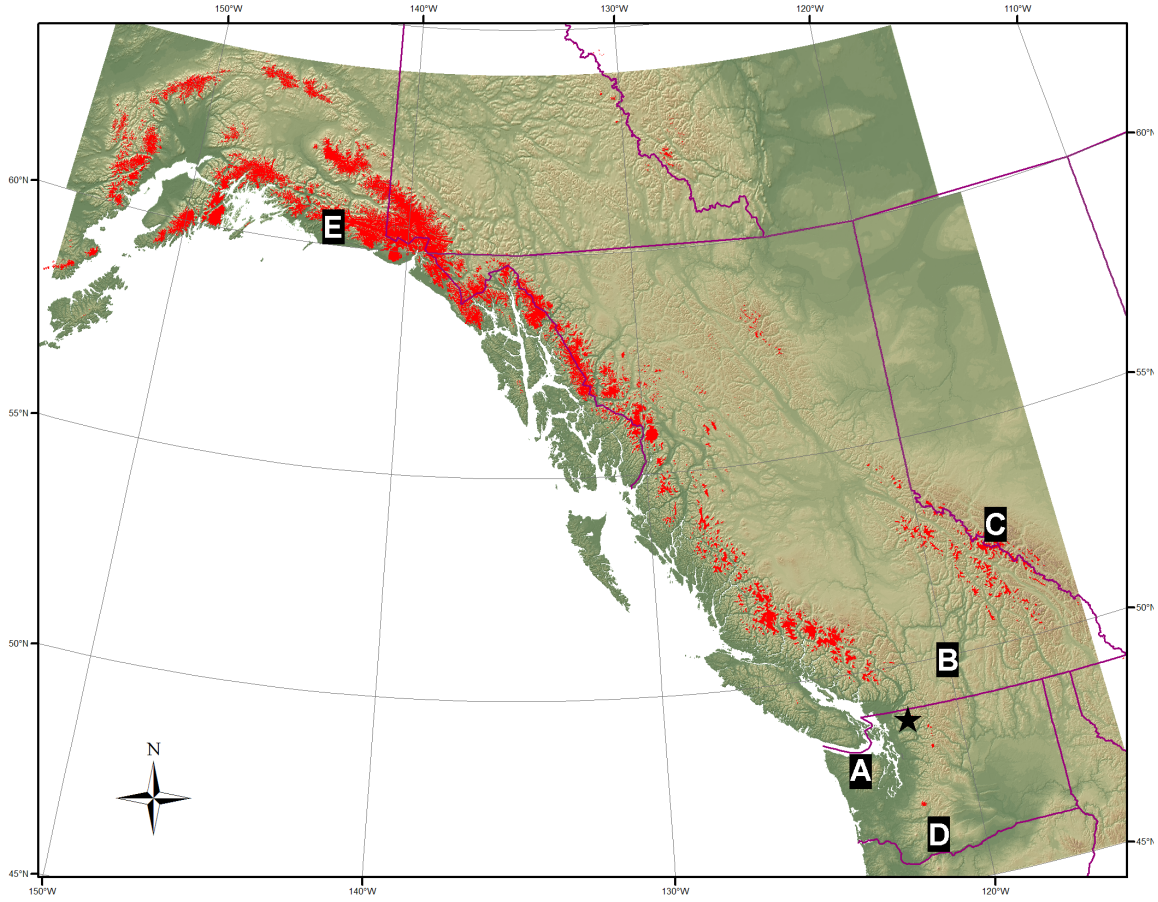

Figure 1. Glaciers in the Pacific Northwest shown in red. Data from the global land ice monitoring from space (GLIMS) project (http://www.glims.org/_ The location of Mt Bake is denoted with an asterisk. Also indicated in the figure are the locations where glacier model sensitivity is tested. Figure courtesy Harvey Greenberg).

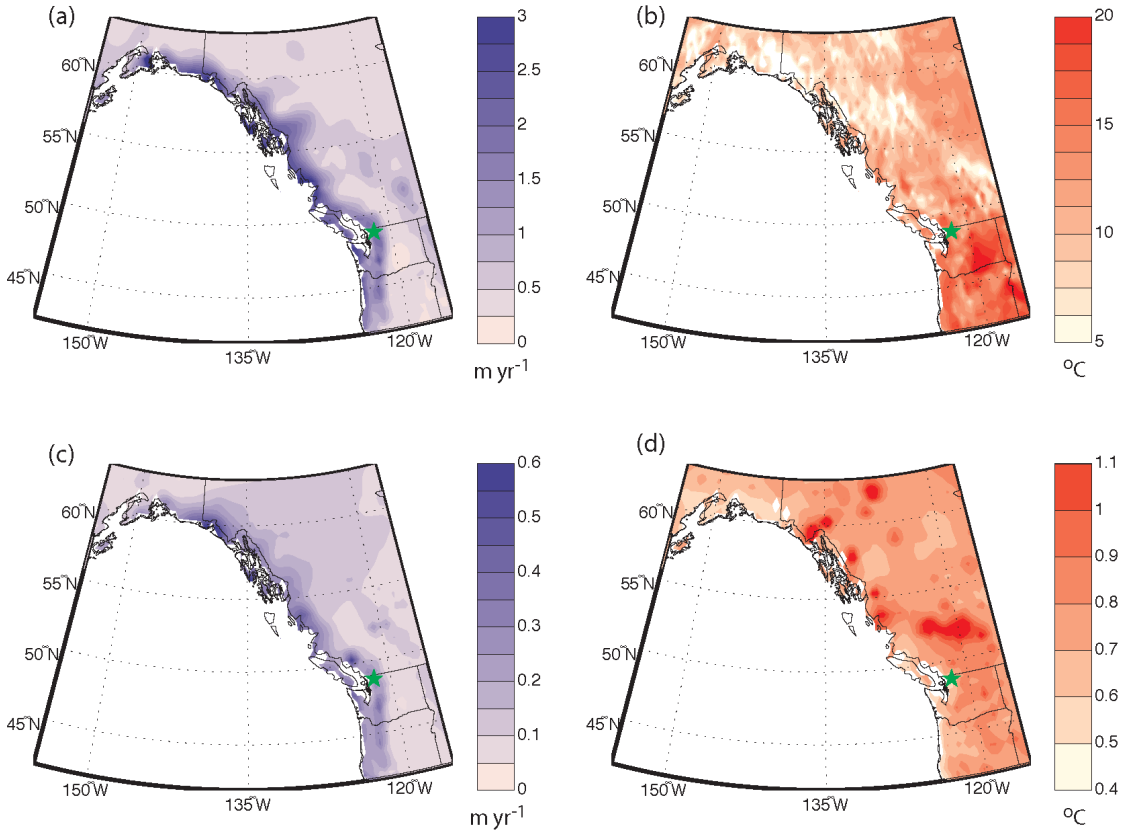

Figure 2. Climate mean and variability in the Pacific Northwest from LW50. a) Mean annual precipitation, in m yr^{-1}; b) Mean melt-season (JJAS) temperature in °C.; c) interannual standard deviation of mean annual precipitation, in m yr^{-1}; and d) interannual standard deviation of melt-season temperature, in °C.

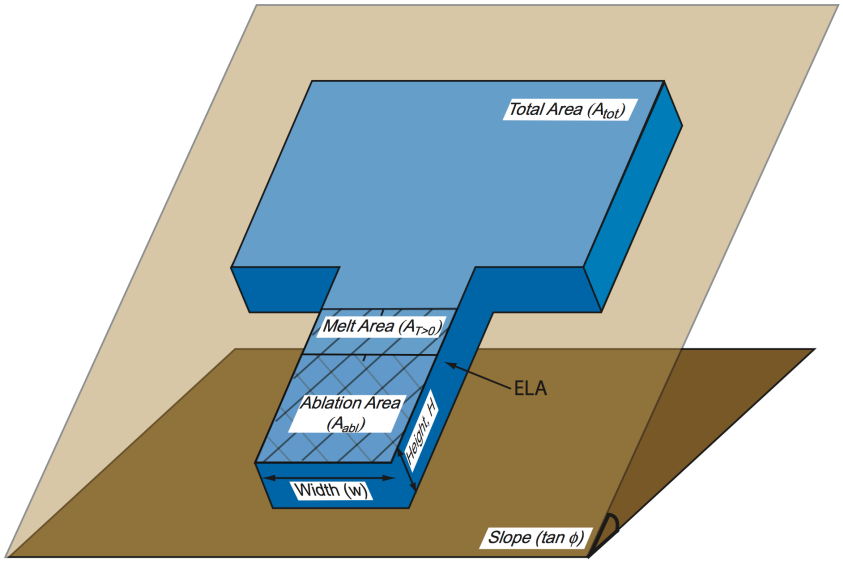

Figure 3: Schematic of linear glacier model, based on Johanneson et. al. (1989). Precipitation falls over the entire surface of the glacier (A_{tot}). Melt is linearly proportional to the temperature, which, in turn, decreases linearly as the tongue of the glacier recedes up the linear slope (tan ϕ), and increases as the glacier advances downslope. Melt occurs over the lower reaches of the glacier where melt-season temperature exceeds 0 ($A_{T>0}$), and net mass loss occurs over a smaller area where melting exceeds precipitation (A_{abl}), The upper boundary of this latter region is known as the equilibrium line altitude, (ELA). The height (H) of the glacier, and the width of the ablation area (w) remain constant by assumption.

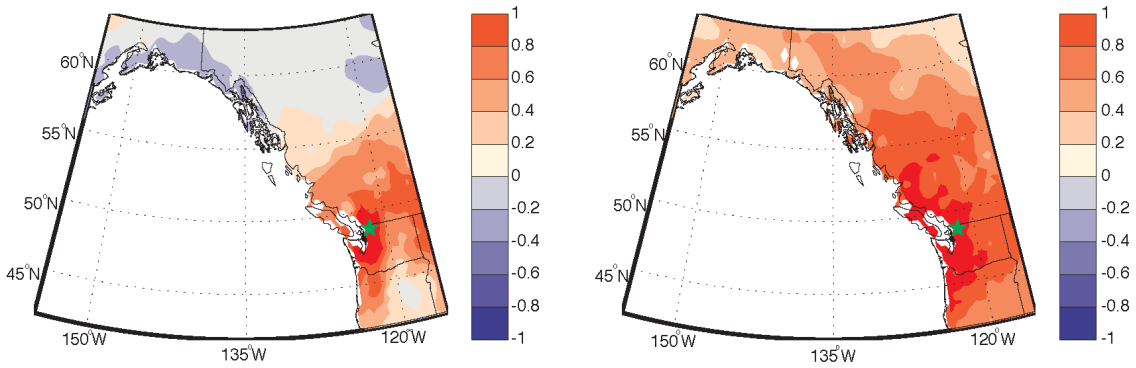

Figure 4. a) Correlation in annual mean precipitation between each grid point and Mt. Baker, from LW50 dataset. Note the dipole of correlations between Alaska and Washington.; b) as in a), but for the correlation of melt-season temperature. Note the widespread correlation of uniform sign over the region. Correlations exceeding about 0.28 would pass a t-test at greater than 95% confidence.

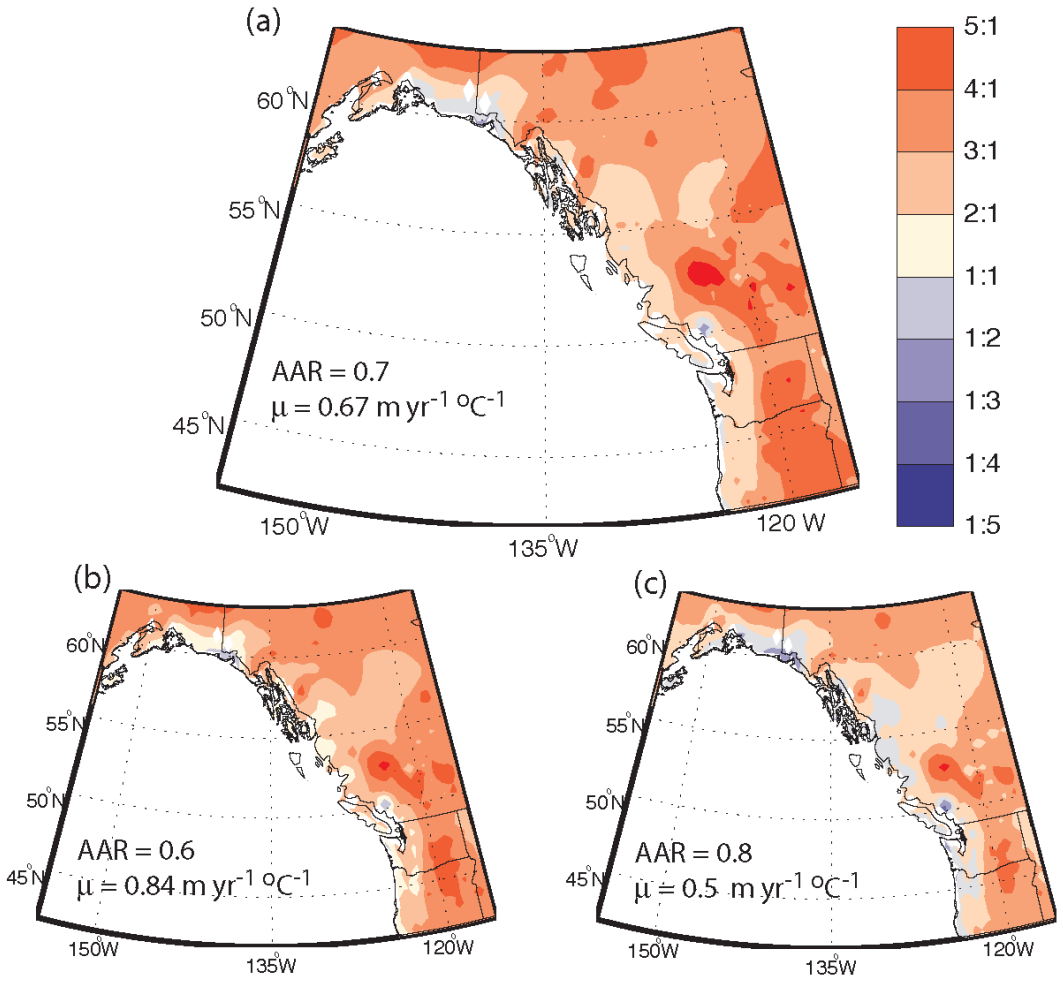

Figure 5. Ratio of sensitivities to temperature and precipitation for a typical glacier geometry at each grid point, for different choice of model parameters. Warm colors denote temperature sensitivity, while cool colors denote sensitivity to precipitation. Panel a) has the standard parameters. Panel b) has the largest ablation area and melt rate factor, and panel c) has the smallest values of the ablation area and melt rate factor.

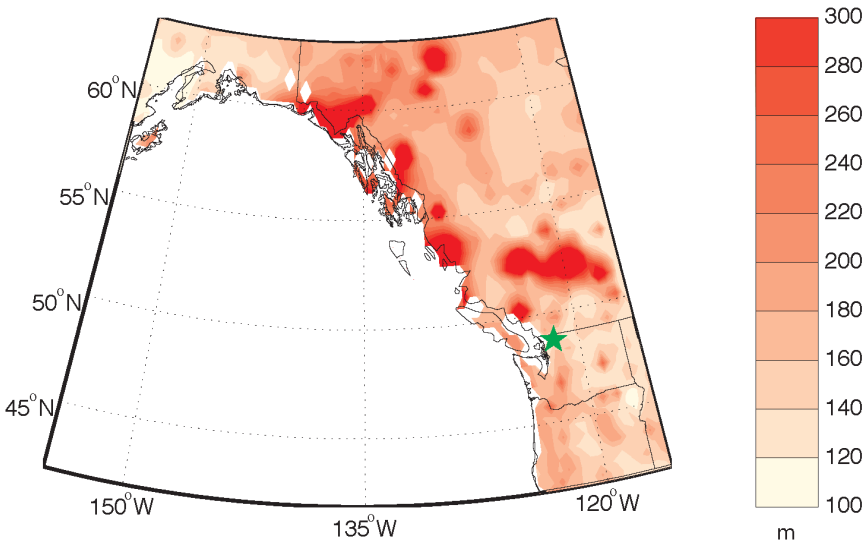

Figure 6: Standard deviations of glacier length at each grid point if a typical glacier exists at each grid point. Standard deviations are calculated from (17). Large standard deviations in length are driven by large standard deviations in either precipitation or temperature (compare with Figure 2).

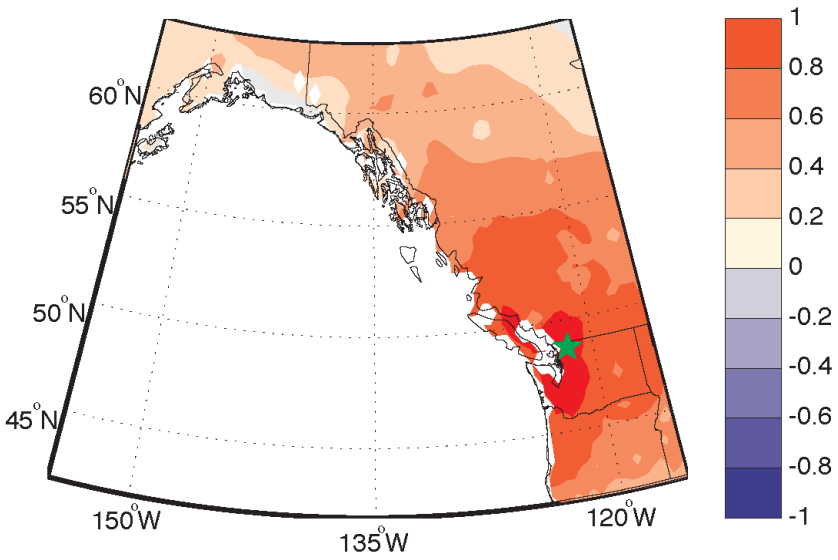

Figure 7: Correlations between a typical glacier glacier at each grid point and at Mt. Baker, calculated from (9).

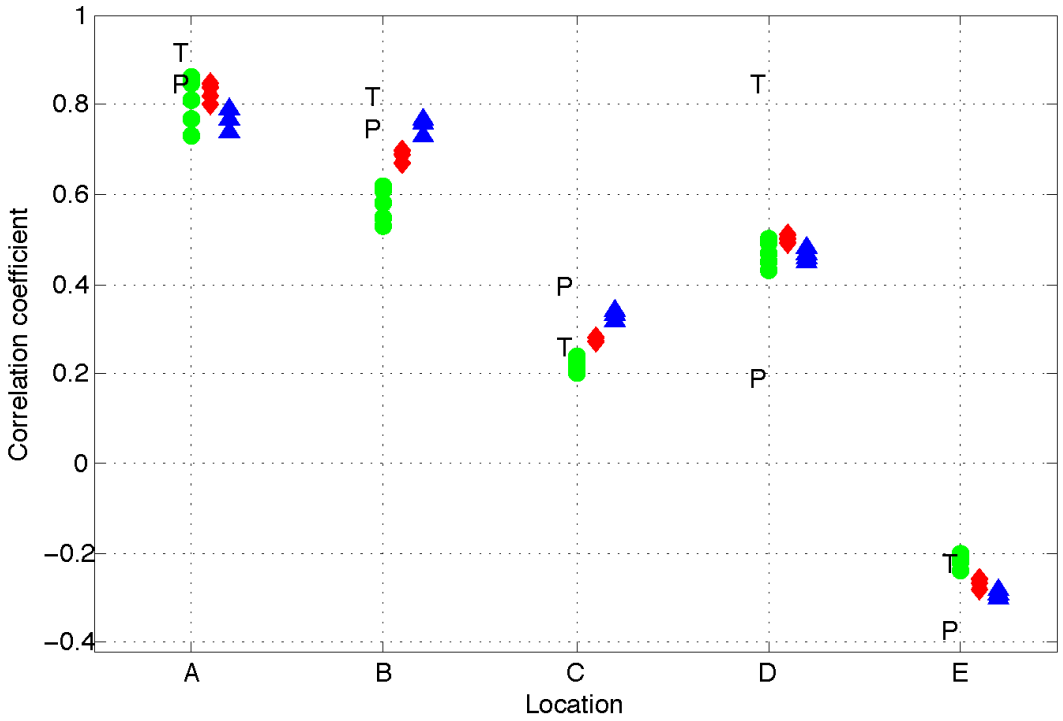

Figure 8: Sensitivity test of correlations at selected locations (see Figure 5b), to varying the glacier geometry and parameters. T and P denote melt-season temperature and annual precipitation correlations, respectively, between that location point and Mt. Baker. The colored symbols represent the correlation of glacier length between that location and Mt. Baker, and the range arises from using the five different parameter sets applying to the different Mt. Baker glaciers (given in Table 1)., Finally the different colors mean a different AAR was used: green (AAR =0.6), red (AAR = 0.7), and (AAR = 0.8).

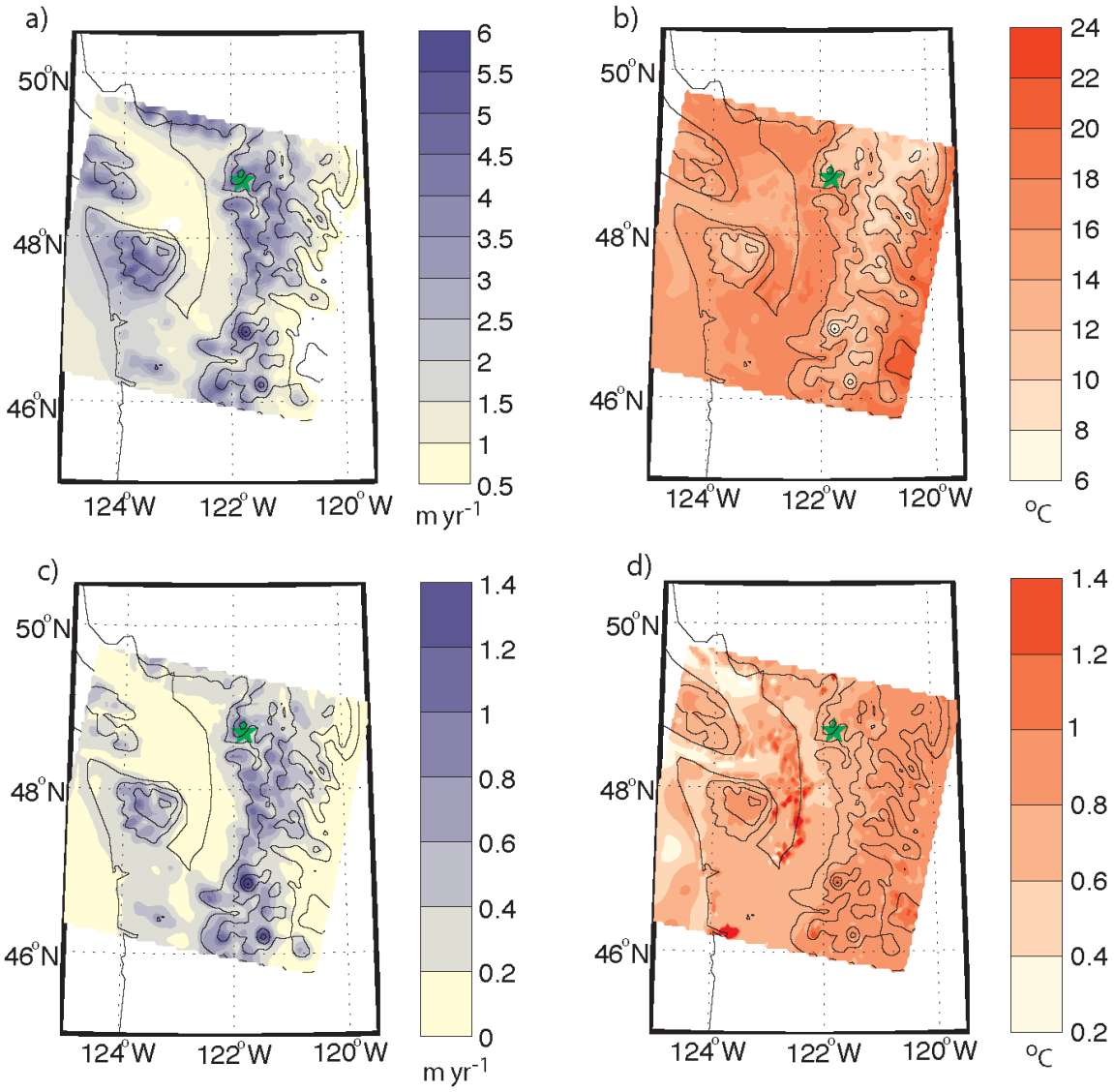

Figure 9: Archived output from MM5 numerical weather prediction for the Pacific Northwest at 4 km scale: a) Mean annual precipitation; b) Mean melt-season temperature; c) Standard deviation of precipitation; and d) standard deviation of melt-season temperature. Contours of the model surface elevation are also plotted every 500 m, and the location of Mt. Baker is indicated with an asterisk. Note the small-scale patterns of climate associated with the mountainous terrain, in particular the high rates of orographic precipitation.

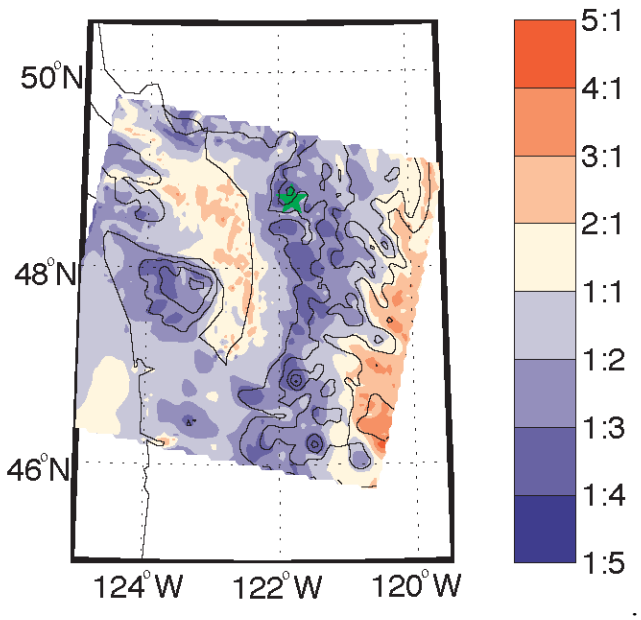

Figure 10. The ratio of sensitivities to temperature and precipitation of a glacier length with a typical Mt. Baker-like geometry, calculated at every model grid point from (16). Blue indicates a greater sensitivity to precipitation. The mountainous regions of the Olympics and Cascades, where glaciers in the region actually exist, are dominated by sensitivity to variation in the precipitation

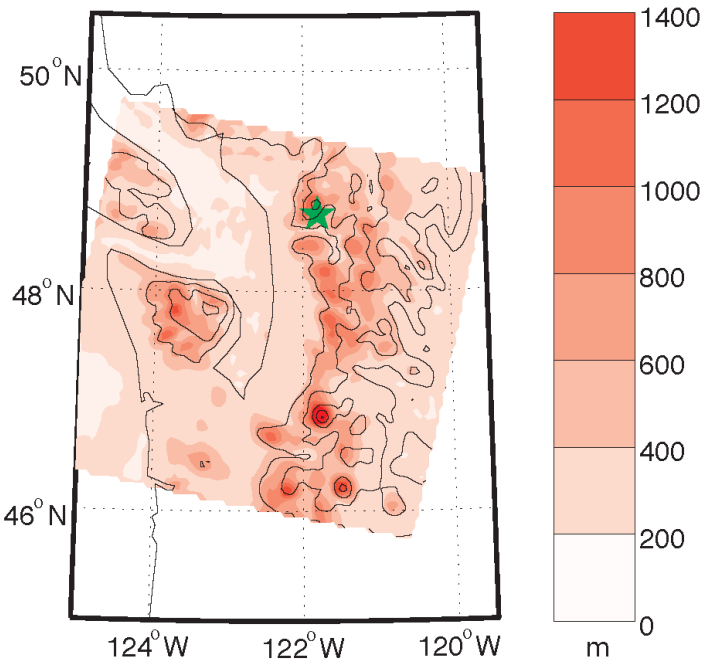

Figure 11: The standard deviation of glacier length calculated from (17) using the 4 km resolution MM5 output. This fine-resolution scale shows that in the mountainous regions where glaciers exist, the standard deviation in glacier length is much higher than in the lower elevations. The high standard deviations are driven by the high variability in precipitation there.